

Checking Potassium origin of new emission line at 3.5 keV with K XIX line complex at 3.7 keV

Dmytro Iakubovskiy^{1*}

¹Bogolyubov Institute of Theoretical Physics, Metrologichna Str. 14-b, 03680, Kyiv, Ukraine

Accepted XXX. Received YYY; in original form ZZZ

ABSTRACT

Whether the new line at ~ 3.5 keV, recently detected in different samples of galaxy clusters, Andromeda galaxy and central part of our Galaxy, is due to Potassium emission lines, is now unclear. By using the latest astrophysical atomic emission line database AtomDB v. 3.0.2, we show that the most prospective method to directly check its Potassium origin will be the study of K XIX emission line complex at ~ 3.7 keV with future X-ray imaging spectrometers such as Soft X-ray spectrometer on-board *Astro-H* mission or microcalorimeter on-board *Micro-X* sounding rocket experiment. To further reduce the remaining (factor $\sim 3 - 5$) uncertainty of the 3.7/3.5 keV ratio one should perform more precise modeling including removal of significant spatial inhomogeneities, detailed treatment of background components, and further extension of the modeled energy range.

Key words: X-rays: general – line: identification – techniques: imaging spectroscopy

1 INTRODUCTION

In 2014, new emission line at ~ 3.5 keV has been detected in X-ray spectra of various galaxy clusters and Andromeda galaxy (Bulbul et al. 2014b; Boyarsky et al. 2014c). Using publicly available emission line database AtomDB v.2.0.2 (Foster et al. 2012), Bulbul et al. (2014b) showed that intensities of individual atomic emission lines near 3.5 keV in spectra of different combinations of galaxy clusters are smaller by a factor ≥ 10 than the detected flux of the extra line. Boyarsky et al. (2014c) showed that the radial profile of the new line in Perseus galaxy outskirts does not coincide with expected astrophysical line distribution. In addition, Boyarsky et al. (2014a) showed that the total expected flux from K XVIII lines at ~ 3.5 keV is more than an order of magnitude smaller than the observed new line. So Bulbul et al. (2014b); Boyarsky et al. (2014c) argued against the astrophysical line origin of the detected line and suggested instead the radiative decay of dark matter particles. This new hypothesis was found consistent with subsequent detection of the 3.5 keV line in the Galactic Centre region (Boyarsky et al. 2014b; Lovell et al. 2014).

An alternative viewpoint has been presented in Riemer-Sorensen (2014); Jeltema & Profumo (2015, 2014); Carlson et al. (2015), see also Boyarsky et al. (2014a); Bulbul et al. (2014a); Iakubovskiy (2014) for discussion. In Riemer-Sorensen (2014), no extra line in *XMM-Newton*/EPIC spectrum of the Galactic Centre region is found after adding an extra line with an arbitrary normalization at 3.51 keV (the mean energy of

K XVIII line emission at ~ 3.5 keV). Based on AtomDB v.2.0.2, Jeltema & Profumo (2015) compared intensities of bright emission lines from both the Galactic Centre region and the combined galaxy cluster sample of Bulbul et al. (2014b) and explained the observed 3.5 keV line with mild ($\lesssim 3$) K/Ca ratio with respect to Solar value. By studying Galactic Centre and Perseus cluster morphologies in different energy bands, Carlson et al. (2015) found positive correlation of 3.45–3.60 keV band with other bands with prominent Ar and Ca lines and no correlation with smooth dark matter profile. Based on these findings, Jeltema & Profumo (2015, 2014) argued that the line at 3.5 keV in Galactic Centre, the central part of the Perseus cluster and the combined galaxy cluster dataset of Bulbul et al. (2014b) is a mixture of K XVIII lines at 3.47 and 3.51 keV and therefore may have a purely astrophysical origin.

The goal of this paper is to further investigate possible Potassium origin of the ~ 3.5 keV line. If the new line is due to Potassium emission lines in multi-temperature plasma as suggested by Jeltema & Profumo (2015, 2014); Carlson et al. (2015), several other Potassium lines should also be excited at keV energies and their intensities can be predicted using the method described in Sec. 2. In Sec. 3 we tabulated positions and expected intensities of these lines, and compared them with measured line properties in Perseus cluster and Galactic Centre. Our conclusions are summarized in Sec. 4.

* E-mail: yakubovskiy@bitp.kiev.ua

2 D. Iakubovskiy

2 METHODS

The line flux for a multi-temperature APEC (Smith et al. 2001) model with electron temperatures $T_{e,i}$ is

$$F[\text{ph cm}^{-2} \text{s}^{-1}] \equiv 10^{14} \sum_i [\epsilon(T_{e,i}) \times A_i \times N_i], \quad (1)$$

where $\epsilon(T_{e,i})$ is the line emissivity (in $\text{cm}^3 \text{s}^{-1}$), A_i is the abundance of the line emitting element (with respect to Solar values adopted in Anders & Grevesse (1989)), $N_i = \frac{10^{-14}}{4\pi D_A^2(1+z)^2} \int n_e n_H dV$ is the APEC model normalization (in cm^{-5}), D_A is the angular diameter distance to the source (in cm), z is the source redshift, $\int n_e n_H dV$ is the plasma emission measure (in cm^{-3}) of i -th thermal component. Using (1), one can determine the astrophysical flux of the new line from measured fluxes of bright astrophysical lines emitted by *the other* elements. Indeed, if one measures the flux of the bright “reference” line

$$F^{(\text{ref})} = 10^{14} \sum_i [\epsilon^{(\text{ref})}(T_{e,i}) \times A_i^{(\text{ref})} \times N_i], \quad (2)$$

one can rewrite the flux of the new line

$$F^{(\text{new})} = 10^{14} \sum_i [\epsilon^{(\text{new})}(T_{e,i}) \times A_i^{(\text{new})} \times N_i] \quad (3)$$

through $F^{(\text{ref})}$

$$F^{(\text{new})} = F^{(\text{ref})} \times \frac{\sum_i [\epsilon^{(\text{new})}(T_{e,i}) \times A_i^{(\text{new})} \times N_i]}{\sum_i [\epsilon^{(\text{ref})}(T_{e,i}) \times A_i^{(\text{ref})} \times N_i]}. \quad (4)$$

Assuming abundances of all components to be the same ($A_i^{(\text{ref})} = A^{(\text{ref})}$, $A_i^{(\text{new})} = A^{(\text{new})}$), one obtains more convenient expression used in Bulbul et al. (2014b); Jeltema & Profumo (2015); Bulbul et al. (2014a); Jeltema & Profumo (2014)

$$F^{(\text{new})} = F^{(\text{ref})} \times \frac{A^{(\text{new})}}{A^{(\text{ref})}} \times \frac{\sum_i [\epsilon^{(\text{new})}(T_{e,i}) \times N_i]}{\sum_i [\epsilon^{(\text{ref})}(T_{e,i}) \times N_i]}. \quad (5)$$

The predicted line flux $F^{(\text{new})}$ linearly depends on the Potassium-to-metal abundance ratio $A^{(\text{new})}/A^{(\text{ref})}$ which is not measured directly (due to absence of strong K lines) and has to be determined further, e.g. from chemical evolution models (Timmes et al. 1995; Romano et al. 2010) or optical (Shimansky et al. 2003; Andrievsky et al. 2010) or X-ray (Phillips et al. 2015) line studies. Possible difference of $A_i^{(\text{new})}/A_i^{(\text{ref})}$ ratios among components in multi-temperature plasma (e.g. due to supernova ejecta) not discussed in Bulbul et al. (2014b); Jeltema & Profumo (2015); Bulbul et al. (2014a); Jeltema & Profumo (2014) will introduce further uncertainties to this method. As a result, it is very hard to robustly confirm or rule out the astrophysical origin of the new line.

Following Bulbul et al. (2014a); Jeltema & Profumo (2014), we avoid the above-mentioned uncertainty by studying emission lines of *the same* element so that $A^{(\text{new})} \equiv A^{(\text{ref})}$ and (4) simplifies:

$$F^{(\text{new})} = F^{(\text{ref})} \times \frac{\sum_i [\epsilon^{(\text{new})}(T_{e,i}) \times N_i]}{\sum_i [\epsilon^{(\text{ref})}(T_{e,i}) \times N_i]}. \quad (6)$$

To calculate line emissivities, we used the latest available version of astrophysical atomic emission line database AtomDB v.3.0.2.

It contains much larger dataset of atomic emission lines of all elements from Hydrogen to Nickel (excluding Lithium and Beryllium) and updated information about line emissivities. Similar to AtomDB v2.0.2 used in previous papers (Bulbul et al. 2014b; Jeltema & Profumo 2015; Boyarsky et al. 2014a; Bulbul et al. 2014a; Jeltema & Profumo 2014), it is restricted to lines with emissivity $> 10^{-20} \text{ ph cm}^3/\text{s}$.

To account the finite energy resolution of imaging spectrometers, we broadened each emission line with a Gaussian shape

$$f(E) = \frac{1}{2\pi\sigma^2} \exp\left(-\frac{(E - E_0)^2}{2\sigma^2}\right),$$

where E_0 is the line position, σ is a energy dispersion (note that, for the Gaussian line full width at half-maximum (FWHM) of the line is defined as $2\sigma\sqrt{2\log(2)} \approx 2.35\sigma$). According to Fig. 5.24 of Iakubovskiy (2013), for the EPIC imaging spectrometers on-board XMM-Newton mission $\sigma_{\text{EPIC}} \approx 60 \text{ eV}$ at $E = 3 - 4 \text{ keV}$. For comparison, we used future Astro-H/SXS spectrometer with FWHM $\lesssim 7 \text{ eV}$ (Mitsuda et al. 2014)¹. Further Doppler broadening gives $\sigma_{\text{SXS}} \lesssim 5 \text{ eV}$ assuming gas bulk velocities for the Galactic Centre and the central part of Perseus cluster $\lesssim 500 \text{ km/s}$ (Tamura et al. 2014; Kitayama et al. 2014; Koyama et al. 2014).

3 RESULTS

The main properties of Potassium emission lines above 1 keV and the adjacent emission lines of the other elements (S, Cl, Ar, Ca) are summarized in Table 1. In addition to K XVIII lines at 3.476, 3.496, 3.498, 3.500 and 3.515 keV, potentially responsible for the new 3.5 keV line, it also contains two rather bright K XIX lines at 3.700 and 3.706 keV surrounded by rather strong Ar XVII lines at 3.683-3.685 keV, and two very weak (~ 10 times fainter than the K XVIII line complex at 3.51 keV) Potassium lines above 4 keV: K XVIII line at 4.125 keV and K XIX line at 4.389 keV. Below 1 keV, all Potassium lines fall into “line forest” region and are strongly subdominant.

The emissivities of K XVIII (3.476-3.515 keV), K XIX (3.700-3.706 keV) and Ar XVII (3.683-3.685 keV) line complexes as functions of electron temperature T_e are shown in Fig. 1, see also Fig. 8 of Urban et al. (2015) for AtomDB v. 2.0.2. For $T_e \gtrsim 3 \text{ keV}$, 3.700-3.706 keV K XIX line signal becomes comparable or stronger than that of 3.476-3.515 keV K XVIII lines which should lead to significant detection of $\sim 3.7 \text{ keV}$ line.

Fig. 1 shows that the 3.7/3.5 keV line ratio strongly depends on exact temperatures of individual components in thermal plasma. We illustrate this uncertainty with different models parameters of the Galactic Centre and Perseus cluster spectra. Jeltema & Profumo (2015) considered three models of Galactic Centre region: two-component with $T_{e,1} = 1 \text{ keV}$, $T_{e,2} = 7 \text{ keV}$ and $N_1/N_2 = 4$; two-component with $T_{e,1} = 0.8 \text{ keV}$, $T_{e,2} = 8 \text{ keV}$ and $N_1/N_2 = 3$; three-component with $T_{e,1} = 0.8 \text{ keV}$, $T_{e,2} = 2 \text{ keV}$, $T_{e,3} = 8 \text{ keV}$ and $N_1 : N_2 : N_3 = 0.17 : 1.0 : 0.075$. The corresponding 3.7/3.5 keV line ratios are 0.084, 0.189 and 0.276, respectively. Bulbul et al. (2014b) modeled MOS spectra of Perseus cluster and found $T_{e,1} = 3.6 \pm 0.6 \text{ keV}$, $N_1 = 15.7 \pm 7.8 \times 10^{-2} \text{ cm}^{-5}$,

¹ Similar energy resolution will be reached in Micro-X sounding rocket experiment (Figueroa-Feliciano et al. 2015) planning to observe the innermost part of our Galaxy.

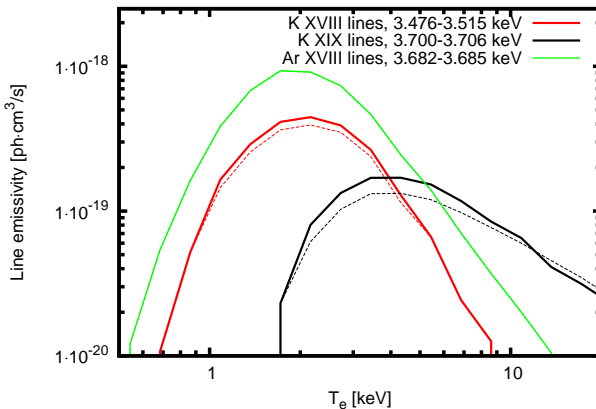


Figure 1. Emissivities of K XVIII (3.476–3.515 keV), K XIX (3.700–3.706 keV) and Ar XVIII (3.683–3.685 keV) line complexes as function of electron temperature T_e . The K and Ar abundances are set to Solar (Anders & Grevesse 1989). Solid and dashed lines show contributions from AtomDB v3.0.2 and AtomDB v2.0.2, respectively (no difference between these AtomDB versions for Ar XVIII, < 15% difference for K XVIII and < 30% difference for K XIX).

$T_{e,2} = 7.6 \pm 0.7$ keV, $N_2 = 44.0 \pm 6.8 \times 10^{-2}$ cm⁻⁵ which gives 3.7/3.5 keV line ratio $1.77^{+4.9}_{-0.46}$.

In addition to the factor $\sim 3\text{--}5$ uncertainty in 3.7/3.5 keV line ratio for the Galactic Center and Perseus cluster, another uncertainty comes from strong contribution of Ar XVII lines at 3.683–3.685 keV located only ~ 20 eV away from 3.700–3.706 keV K XIX line complex. We visualize the relative contributions of these lines by broadening line emissivities for Galactic Centre (three-component model of Jeltema & Profumo (2015)) and Perseus cluster (best-fit two-component model of Bulbul et al. (2014b) for combined MOS spectrum) with XMM-Newton/EPIC energy resolution, see Fig. 2 for details. In both sources, the S, Ar, Cl and K abundances ratio are set to 1/3 : 1 : 1 : 3, close to that obtained by Jeltema & Profumo (2015) for Galactic Centre region. This uncertainty can be avoided by using future instruments with higher energy resolution, see Fig. 3 for the planned Astro-H/SXS instrument and Micro-X sounding rocket experiment.

Existing stacked X-ray spectra of nearby galaxies and galaxy groups (Iakubovskyi 2013; Anderson et al. 2014) did not allow to draw any conclusion about the astrophysical origin of the 3.5 keV line. Indeed, a simple (but abundance-dependent) estimate of Ar XVIII lines strength at 3.683–3.685 keV (dominating at low electron temperatures $T_e < 1$ keV expected from Anderson et al. (2014) according to Fig. 1) can be made by using luminous S XV line complex at ~ 2.45 keV, see e.g. Fig. 3 of Bulbul et al. (2014a) for AtomDB 2.0.2. An estimate with the newest AtomDB 3.0.2 gives the expected 2.45keV/3.68keV line flux ratio $> 170 \times$ Abund[S]/Abund[Ar] for $T_e < 1$ keV. More precise (abundance-independent) estimate can be made using the brightest Ar XVII line complex at 3.10–3.14 keV which gives 3.14keV/3.68keV line flux ratio > 20 for $T_e < 1$ keV.

4 CONCLUSIONS

Determination of Potassium origin of the new line at ~ 3.5 keV in thermal multi-component plasma suffers from several uncertainties, the most significant of them are the uncertainties of the

plasma temperatures and of the relative element abundances among the thermal components. Future study of K XIX emission lines at ~ 3.7 keV with high-resolution imaging spectrometers such as SXS spectrometer on-board *Astro-H* mission (Mitsuda et al. 2014) or microcalorimeter on-board *Micro-X* sounding rocket experiment (Figueroa-Feliciano et al. 2015) can completely avoid the second uncertainty².

To reduce the remaining uncertainty, one has to improve the thermal continuum modeling including removal of significant spatial inhomogeneities, detailed treatment of background components (such as instrumental background and residual soft proton flares for *XMM-Newton/EPIC*), and further extension of the modeled energy range (possibly including the data from other instruments).

ACKNOWLEDGEMENTS

The author thanks Michael E. Anderson for his comment about the detection of astrophysical lines in stacked galaxy spectra. This work was supported by part by the SCOPE grant IZ7370-152581 and the Program of Cosmic Research of the National Academy of Sciences of Ukraine.

REFERENCES

- Anders E., Grevesse N., 1989, *Geochim. Cosmochim. Acta*, **53**, 197
- Anderson M. E., Churazov E., Bregman J. N., 2014, preprint, ([arXiv:1408.4115](https://arxiv.org/abs/1408.4115))
- Andrievsky S. M., Spite M., Korotin S. A., Spite F., Bonifacio P., Cayrel R., François P., Hill V., 2010, *A&A*, **509**, A88
- Boyarsky A., Franse J., Iakubovskyi D., Ruchayskiy O., 2014b, preprint, ([arXiv:1408.2503](https://arxiv.org/abs/1408.2503))
- Boyarsky A., Franse J., Iakubovskyi D., Ruchayskiy O., 2014a, preprint, ([arXiv:1408.4388](https://arxiv.org/abs/1408.4388))
- Boyarsky A., Ruchayskiy O., Iakubovskyi D., Franse J., 2014c, *Physical Review Letters*, **113**, 251301
- Bulbul E., Markevitch M., Foster A. R., Smith R. K., Loewenstein M., Randall S. W., 2014a, preprint, ([arXiv:1409.4143](https://arxiv.org/abs/1409.4143))
- Bulbul E., Markevitch M., Foster A., Smith R. K., Loewenstein M., Randall S. W., 2014b, *ApJ*, **789**, 13
- Carlson E., Jeltema T., Profumo S., 2015, *JCAP*, **2**, 9
- Figueroa-Feliciano E., et al., 2015, preprint, ([arXiv:1506.05519](https://arxiv.org/abs/1506.05519))
- Foster A. R., Ji L., Smith R. K., Brickhouse N. S., 2012, *ApJ*, **756**, 128
- Iakubovskyi D., 2013, PhD thesis, Instituut-Lorentz for Theoretical Physics
- Iakubovskyi D. A., 2014, Advances in Astronomy and Space Physics, **4**, 9
- Jeltema T., Profumo S., 2014, preprint, ([arXiv:1411.1759](https://arxiv.org/abs/1411.1759))
- Jeltema T., Profumo S., 2015, *MNRAS*, **450**, 2143
- Kitayama T., et al., 2014, preprint, ([arXiv:1412.1176](https://arxiv.org/abs/1412.1176))
- Koyama K., et al., 2014, preprint, ([arXiv:1412.1170](https://arxiv.org/abs/1412.1170))
- Lovell M. R., Bertone G., Boyarsky A., Jenkins A., Ruchayskiy O., 2014, preprint, ([arXiv:1411.0311](https://arxiv.org/abs/1411.0311))
- Mitsuda K., et al., 2014, in Society of Photo-Optical Instrumentation Engineers (SPIE) Conference Series. p. 2, doi:[10.1117/12.2057199](https://doi.org/10.1117/12.2057199)
- Phillips K. J. H., Sylwester B., Sylwester J., 2015, preprint, ([arXiv:1507.04619](https://arxiv.org/abs/1507.04619))
- Riemer-Sorensen S., 2014, preprint, ([arXiv:1405.7943](https://arxiv.org/abs/1405.7943))
- Romano D., Karakas A. I., Tosi M., Matteucci F., 2010, *A&A*, **522**, A32
- Shimansky V. V., Bikmaev I. F., Galeev A. I., Shimanskaya N. N., Ivanova D. V., Sakhibullin N. A., Musaev F. A., Galazutdinov G. A., 2003, *Astronomy Reports*, **47**, 750

² If the new line position resolved by the future spectrometers falls off K XVIII lines that will be the clear signature of its *non-Potassium* origin.

Position [eV]	Ion	Transition	T_e range [keV]	$T_{e,max}$ [keV]	$\epsilon_{max}/\epsilon_{2.16}/\epsilon_{4.32}$ [$10^{-20}\text{ph cm}^3/\text{s}$]
3423.78	S XVI	38 → 1	1.08–10.8	2.16	6.8/6.8/3.9
3424.84	S XVI	39 → 1	1.08–21.6	2.16	13.8/13.8/9.4
3440.48	S XVI	51 → 1	1.37–8.62	2.16	3.9/3.9/2.2
3440.52	S XVI	52 → 1	1.08–13.7	2.16	8.7/8.7/6.0
3443.61	Cl XVI	31 → 1	1.08–2.72	1.72	3.0/2.4/—
3451.92	S XVI	66 → 1	1.37–6.84	2.16	2.9/2.9/1.9
3451.95	S XVI	67 → 1	1.37–10.8	2.16	5.1/5.1/3.4
3460.11	S XVI	83 → 1	1.72–5.44	2.16	2.1/2.1/1.4
3460.13	S XVI	84 → 1	1.37–6.84	2.16	3.0/3.0/2.0
3475.94	K XVIII	2 → 1	0.862–5.44	2.16	11.8/11.8/3.5
3496.43	K XVIII	4 → 1	1.08–3.43	2.16	3.4/3.4/—
3497.78	K XVIII	5 → 1	1.08–4.32	2.16	4.8/4.8/1.3
3500.24	K XVIII	6 → 1	1.08–3.43	2.16	2.7/2.7/—
3508.66	Cl XVII	5 → 1	1.72–6.84	2.72	2.6/2.3/2.0
3509.79	Cl XVII	8 → 1	1.37–13.7	2.72	5.8/5.0/3.9
3514.99	K XVIII	7 → 1	0.684–8.62	2.16	21.9/21.9/8.1
3521.93	Cl XVI	41 → 1	1.72–1.72	1.72	1.1/—/—
3616.91	Ar XVI	10078 → 3	0.544–3.43	1.37	9.4/5.0/—
3617.65	Ar XVI	10077 → 2	0.684–2.72	1.37	3.6/1.9/—
3682.78	Ar XVII	11 → 1	1.08–3.43	1.72	3.8/3.4/—
3684.52	Ar XVII	13 → 1	0.544–13.7	1.72	89.5/88.0/24.5
3700.08	K XIX	3 → 1	2.16–10.8	3.43	3.8/1.9/3.7
3701.19	Cl XVII	13 → 1	2.16–4.32	2.72	1.5/1.3/1.1
3705.97	K XIX	4 → 1	1.72–34.3	4.32	13.3/6.2/13.3
3787.74	Ar XVI	10125 → 3	1.37–1.37	1.37	1.0/—/—
3788.9	Ar XVI	10126 → 2	1.08–1.72	1.08	1.2/—/—
3789.25	Ar XVI	10127 → 3	0.862–2.16	1.08	2.3/1.3/—
4100.12	Ca XX	3 → 1	1.37–68.4	4.32	109.7/28.9/109.7
4105.44	Ca XIX	10067 → 23	2.16–5.44	3.43	1.9/1.2/1.6
4105.57	Ca XIX	10027 → 13	2.16–5.44	3.43	2.4/1.5/2.0
4105.84	Ca XIX	10021 → 9	2.72–4.32	3.43	1.2/—/1.0
4106.25	Ca XIX	10118 → 37	3.43–3.43	3.43	1.1/—/—
4107.48	Ca XX	4 → 1	1.37–68.4	4.32	215.2/56.5/215.2
4109.93	Ca XIX	10092 → 30	2.16–4.32	3.43	1.7/1.0/1.4
4110.88	Ca XIX	10037 → 17	2.72–4.32	3.43	1.3/—/1.0
4125.07	K XVIII	17 → 1	1.37–4.32	2.16	2.7/2.7/1.1
4149.72	Ar XVIII	11 → 1	1.72–21.6	3.43	8.6/5.4/7.9
4150.33	Ar XVIII	12 → 1	1.37–34.3	3.43	18.5/11.6/16.9
4249.36	Ar XVIII	18 → 1	1.72–10.8	3.43	3.8/2.4/3.0
4249.67	Ar XVIII	19 → 1	1.72–21.6	3.43	8.3/5.2/7.7
4304.59	Ar XVIII	27 → 1	2.16–6.84	3.43	2.0/1.4/1.8
4304.77	Ar XVIII	28 → 1	1.72–13.7	3.43	4.5/2.8/4.2
4337.19	Ar XVIII	39 → 1	2.72–4.32	3.43	1.2/—/1.1
4337.3	Ar XVIII	39 → 1	2.16–8.62	2.72	2.4/1.7/2.1
4358.41	Ar XVIII	52 → 1	2.72–5.44	3.43	1.5/—/1.4
4372.88	Ar XVIII	67 → 1	3.43–3.43	3.43	1.0/—/—
4388.76	K XIX	8 → 1	2.72–8.62	4.32	1.8/—/1.8

Table 1. Emission lines at 3.4–3.8 and 4.1–4.5 keV range from AtomDB v3.0.2 database. Level transitions are in AtomDB format. Range of T_e shows when the emissivity of a given line is $> 10^{-20}\text{ph cm}^3/\text{s}$. $T_{e,max}$ and ϵ_{max} indicate the temperature at which maximal emissivity of the line is reached, and the maximal value of the line emissivity; $\epsilon_{2.16}$ and $\epsilon_{4.32}$ are the line emissivities at $T_e = 2.16$ and 4.32 keV.

Smith R. K., Brickhouse N. S., Liedahl D. A., Raymond J. C., 2001, *ApJ*,

[556, L91](#)

Tamura T., et al., 2014, *ApJ*, [782, 38](#)

Timmes F. X., Woosley S. E., Weaver T. A., 1995, *ApJS*, [98, 617](#)

Urban O., Werner N., Allen S. W., Simionescu A., Kaastra J. S., Strigari

L. E., 2015, *MNRAS*, [451, 2447](#)

This paper has been typeset from a TeX/LaTeX file prepared by the author.

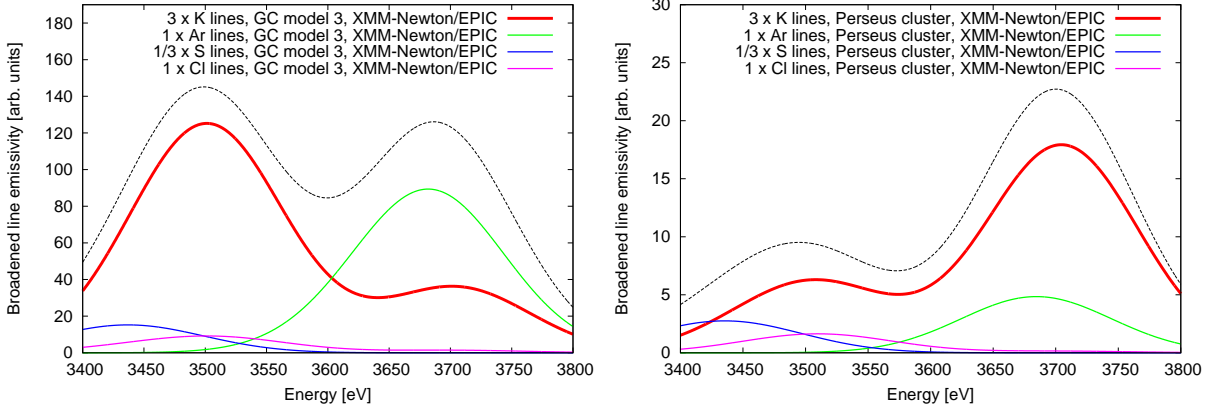


Figure 2. *Left:* Broadened with $\sigma_{XMM} = 60$ eV line emissivities as functions of energy for three-component model of Jeltema & Profumo (2015) of Galactic Centre. The relative S, Ar, Cl and K abundances are set to 1/3 : 1 : 1 : 3, see Sec. 2.2 of Jeltema & Profumo (2015). Thin dashed line shows the total emissivity. *Right:* Broadened line emissivities as functions of energy for the best-fit two-component model of Perseus cluster given by Bulbul et al. (2014b). The relative element abundances in Solar units given by Anders & Grevesse (1989) are the same as in the left Figure.

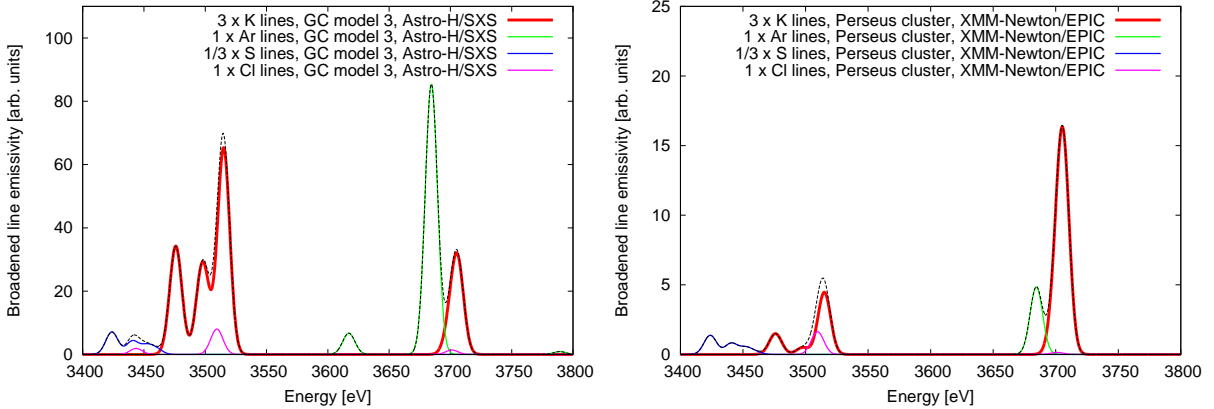


Figure 3. The same as in the previous Figure but broadened with *Astro-H/SXS* or *Micro-X* energy resolution $\sigma_{SXS} = 5$ eV (see text).